

Copyright Notice

This paper was published in [Optics Express] doi:10.1364/OE.18.015426 and is made available as an electronic reprint with the permission of OSA. Systematic or multiple reproduction or distribution to multiple locations via electronic or other means is prohibited and is subject to penalties under law.

(Article begins on next page)

Noise performance of optical fiber transmission links that use non-degenerate cascaded phase-sensitive amplifiers

Zhi Tong,^{1,*} C. J. McKinstrie,² Carl Lundström,¹ Magnus Karlsson,¹ and Peter A. Andrekson¹

¹Photonics Laboratory, Department of Microtechnology and Nanoscience, Chalmers University of Technology, SE-412 96 Göteborg, Sweden

²Bell Laboratories, Alcatel-Lucent, Holmdel, NJ 07733, USA

*zhi.tong@chalmers.se

Abstract: Based on semi-classical theory, the noise performance of a multi-span fiber optical transmission system employing a cascaded phase-insensitive amplifier (PIA) and phase-sensitive amplifiers (PSAs) is investigated. Compared with the pure-PIA and pure-PSA based in-line amplification schemes, the copier + PSA scheme is found to improve the system NF by up to 6 and 3 dB, respectively, in an optimized long-haul fiber link. In addition, this cascaded configuration will significantly relax the requirement for accurate phase- and wavelength-locking which is rigorously needed in the pure-PSA configuration. This scheme is also modulation-format independent. As a proof of concept, the NF of a fiber parametric amplifier based copier + PSA cascade with inter-stage attenuation representing the fiber link is measured, which shows a 1.8-dB total NF improvement over the conventional EDFA cascade.

©2010 Optical Society of America

OCIS codes: (060.2320) Fiber optics amplifiers and oscillators; (190.4380) Nonlinear optics, four-wave mixing.

References and links

1. C. M. Caves, "Quantum limits on noise in linear amplifiers," *Phys. Rev. D Part. Fields* **26**(8), 1817–1839 (1982).
2. J. A. Levenson, K. Bencheikh, D. J. Loring, P. Vidakovic, and C. Simonneau, "Quantum noise in optical parametric amplification: a means to achieve noiseless optical functions," *Quantum Semiclass. Opt.* **9**(2), 221–237 (1997).
3. M. V. Vasilyev, "Phase-sensitive amplification in optical fibers," in *Frontiers in Optics*, Technical Digest (Optical Society of America, 2005), paper FThB1.
4. J. A. Levenson, I. Abram, Th. Rivera, and P. Grangier, "Reduction of quantum noise in optical parametric amplification," *J. Opt. Soc. Am. B* **10**(11), 2233–2238 (1993).
5. D. Levandovsky, M. Vasilyev, and P. Kumar, "Amplitude squeezing of light by means of a phase-sensitive fiber parametric amplifier," *Opt. Lett.* **24**(14), 984–986 (1999).
6. W. Imajuku, A. Takada, and Y. Yamabayashi, "Low-noise amplification under the 3dB noise figure in high-gain phase-sensitive fibre amplifier," *Electron. Lett.* **35**(22), 1954–1955 (1999).
7. W. Imajuku, and A. Takada, "Error-free operation of in-line phase-sensitive amplifier," *Electron. Lett.* **34**(17), 1673–1674 (1998).
8. R. Tang, P. S. Devgan, V. S. Grigoryan, P. Kumar, and M. Vasilyev, "In-line phase-sensitive amplification of multi-channel CW signals based on frequency nondegenerate four-wave-mixing in fiber," *Opt. Express* **16**(12), 9046–9053 (2008), <http://www.opticsinfobase.org/abstract.cfm?URI=oe-16-12-9046>.
9. R. Tang, J. Lasri, P. S. Devgan, V. S. Grigoryan, P. Kumar, and M. Vasilyev, "Gain characteristics of a frequency nondegenerate phase-sensitive fiber-optic parametric amplifier with phase self-stabilized input," *Opt. Express* **13**(26), 10483–10493 (2005), <http://www.opticsinfobase.org/oe/abstract.cfm?uri=oe-13-26-10483>.
10. R. Tang, P. Devgan, V. S. Grigoryan, and P. Kumar, "In-line frequency-non-degenerate phase-sensitive fibre parametric amplifier for fibre-optic communication," *Electron. Lett.* **41**(19), 1072–1074 (2005).
11. Z. Tong, A. Bogris, C. Lundström, C. J. McKinstrie, M. Vasilyev, M. Karlsson, and P. A. Andrekson, "Noise figure measurements in phase-insensitive and phase-sensitive fiber parametric amplifier cascade," in *Optical Fiber Communications Conference*, paper OWT4 (2010).
12. M. E. Marhic, *Fiber optical parametric amplifiers, oscillators and related devices* (Cambridge University, 2007), Chap. 14.

13. M. V. Vasilyev, "Distributed phase-sensitive amplification," *Opt. Express* **13**(19), 7563–7571 (2005), <http://www.opticsinfobase.org/oe/abstract.cfm?uri=OE-13-19-7563>.
14. E. Desuvire, *Erbium-doped fiber amplifiers* (John Wiley and Sons, 1994), Chap. 2.
15. R. Loudon, "Theory of noise accumulation in linear optical-amplifier chains," *IEEE J. Quantum Electron.* **21**(7), 766–773 (1985).
16. C. J. McKinstrie, M. Yu, M. G. Raymer, and S. Radic, "Quantum noise properties of parametric processes," *Opt. Express* **13**(13), 4986–5012 (2005), <http://www.opticsinfobase.org/oe/abstract.cfm?uri=OE-13-13-4986>.
17. C. J. McKinstrie, S. Radic, R. M. Jopson, and A. R. Chraplyvy, "Quantum noise limits on optical monitoring with parametric devices," *Opt. Commun.* **259**(1), 309–320 (2006).
18. C. J. McKinstrie, M. G. Raymer, S. Radic, and M. Vasilyev, "Quantum mechanics of phase-sensitive amplification in a fiber," *Opt. Commun.* **257**(1), 146–163 (2006).
19. P. Kylemark, P.-O. Hedekvist, H. Sunnerud, M. Karlsson, and P. A. Andrekson, "Noise characteristics of fiber optical parametric amplifiers," *J. Lightwave Technol.* **22**(2), 409–416 (2004).
20. P. L. Voss, and P. Kumar, "Raman-effect induced noise limits on $\chi^{(3)}$ parametric amplifiers and wavelength converters," *J. Opt. B Quantum Semiclassical Opt.* **6**(8), S762–S770 (2004).
21. A. Mecozzi, and P. Tombesi, "Parametric amplification and signal-to-noise ratio in optical transmission lines," *Opt. Commun.* **75**(3–4), 256–262 (1990).
22. W. Imajuku, and A. Takada, "Theoretical analysis of system limitation for AM-DD/NRZ optical transmission systems using in-line phase-sensitive amplifiers," *J. Lightwave Technol.* **16**(7), 1158–1170 (1998).
23. A. Takada, and W. Imajuku, "In-line optical phase-sensitive amplifier employing pump laser injection locked to input signal light," *Electron. Lett.* **34**(3), 274–276 (1998).
24. R. Weerasuriya, S. Sygletos, S. K. Ibrahim, R. Phelan, J. O'Carroll, B. Kelly, J. O'Gorman, and A. D. Ellis, "Generation of frequency symmetric signals from a BPSK input for phase sensitive amplification," in *Optical Fiber Communications Conference*, paper OWT6 (2010).
25. G. Baxter, S. Frisken, D. Abakoumov, H. Zhou, I. Clarke, A. Bartos, and S. Poole, "Highly programmable wavelength selective switch based on liquid crystal on silicon switching elements," in *Optical Fiber Communication Conference*, paper OTuF2 (2009).
26. G. Zhou, and F. S. Chau, "Nondispersive optical phase shifter array using microelectromechanical systems based gratings," *Opt. Express* **15**(17), 10958–10963 (2007), <http://www.opticsinfobase.org/oe/abstract.cfm?URI=oe-15-17-10958>.
27. C. J. McKinstrie, H. Kogelnik, R. Jopson, S. Radic, and A. Kanaev, "Four-wave mixing in fibers with random birefringence," *Opt. Express* **12**(10), 2033–2055 (2004), <http://www.opticsinfobase.org/oe/abstract.cfm?URI=oe-12-10-2033>.
28. N. A. Olsson, "Lightwave systems with optical amplifiers," *J. Lightwave Technol.* **7**(7), 1071–1082 (1989).
29. C. Lundström, J. Kakande, P. A. Andrekson, Z. Tong, M. Karlsson, P. Petropoulos, F. Parmigiani, and D. J. Richardson, "Experimental comparison of gain and saturation characteristics of a parametric amplifier in phase-sensitive and phase-insensitive mode," in *European Conference on Optical Communications*, paper Mo. 1.1.1 (2009).
30. Z. Tong, A. Bogris, C. Lundström, C. J. McKinstrie, M. Vasilyev, M. Karlsson and P. A. Andrekson, "Modeling and measurement of noise figure in a cascaded non-degenerate phase-sensitive parametric amplifier," to appear in *Opt. Express*.
31. T. Torounidis, and P. Andrekson, "Broadband single-pumped fiber-optic parametric amplifiers," *IEEE Photon. Technol. Lett.* **19**(9), 650–652 (2007).
32. Z. Tong, A. Bogris, M. Karlsson, and P. A. Andrekson, "Full characterization of the signal and idler noise figure spectra in single-pumped fiber optical parametric amplifiers," *Opt. Express* **18**(3), 2884–2893 (2010), <http://www.opticsinfobase.org/oe/abstract.cfm?URI=oe-18-3-2884>.
33. M. Movassaghi, M. K. Jackson, V. M. Smith, and W. J. Hallam, "Noise figure of erbium-doped fiber amplifiers in saturated operation," *J. Lightwave Technol.* **16**(5), 812–816 (1998).
34. P. L. Voss, K. G. Köprülü, and P. Kumar, "Raman-noise-induced quantum limits for $\chi^{(3)}$ nondegenerate phase-sensitive amplification and quadrature squeezing," *J. Opt. Soc. Am. B* **23**(4), 598–610 (2006).

1. Introduction

As is well known, phase-sensitive amplifiers (PSAs) have the potential to realize noiseless amplification [1], which is a highly attractive characteristic for high-sensitivity photo-detection [2] as well as high-speed optical communications [3]. To date, most PSA experiments have been based on parametric processes in nonlinear crystals [4] or optical fibers [5]. Phase-sensitive (PS) fiber optical parametric amplifiers (FOPAs) have attracted more attention due to their high gain (partly thanks to the use of highly nonlinear fibers, HNLFs) and their compatibility with fiber communication systems. Basically two types of PS-FOPAs have been studied so far: the frequency degenerate (signal and idler frequencies are identical) and non-degenerate (frequencies are different) cases. Degenerate PSAs are more straightforward to realize [6,7], however, the inherent single-channel property limits their potential applications. For example, non-degenerate PSA schemes can realize exponential gain [3] and multi-channel amplification [8] without suffering the guided acoustic-wave

Brillouin scattering, which makes them more promising in practical WDM systems, though rigorous phase- and frequency-locking among the pump, signal and idler waves is required.

Tang *et al.* demonstrated a simple cascaded PSA scheme [9] which generates balanced, phase- and wavelength-locked signal and idler waves from the first phase-insensitive (PI) FOPA, which we refer to as a ‘copier’, since it generates a wavelength-shifted copy of the input signal. They then utilized these waves as the inputs to the following PSA. They also evaluated such a cascaded system with two FOPAs, with 60 km of standard-single-mode-fiber plus 10 km of dispersion-compensating fiber between them, through bit-error-ratio (BER) measurements [10]. The results show that better BERs can be obtained by using the in-line PSAs than conventional PIAs. However, the PSA performance was not fully optimized, but partly degraded by the phase-locked loop. Recently, a lower-than-2-dB noise figure (NF) was measured at the PSA stage of a copier + PSA cascade when considering both signal and idler inputs [11]. Naturally this cascaded PSA scheme can be extended to more stages by simply adding more fiber spools and PSAs after the first copier stage (without removing the idler), as suggested by Marhic [12] and Vasilyev [13]. One may expect that this in-line amplification scheme will have better noise performance than a pure-PIA amplified link, and also that it will have much simpler structure and less cost compared with a pure-PSA system. However, no quantitative investigations on the noise performance of this scheme used in longer links have been reported until now, though extensive research has been done on the signal-to-noise ratio (SNR) performance of the pure-PIA [14] and pure-PSA [13,15,16] amplified multi-span transmission systems. Generally, these results show that, in theory, the latter scheme has a 3-dB noise figure (NF) benefit over the former.

In this paper, we derive the noise formulas of a multi-span fiber optical transmission system employing the aforementioned cascaded copier + PSA scheme for in-line amplification based on a semi-classical theory, which can be shown to be consistent with the quantum theory in the large-photon-number limit. The result shows that the cascaded PSA scheme can improve the system SNR by up to 6 dB and 3 dB compared to the pure-PIA and pure-PSA cases, respectively, in an optimized multi-span, long-haul transmission link, while this NF benefit will decrease or even disappear for a short-distance link. This big improvement relies on taking advantage of the correlated idler wave generated by the copier. The result implies that the cascaded copier + PSA scheme might be more promising for a long-haul transmission system than a pure-PSA link. As a proof of concept, the NF of a PI- and PS-FOPA cascade, with inter-stage attenuation representing the fiber link, is measured, which shows a 1.8-dB total NF improvement over a cascaded EDFA scheme.

2. Semi-classical theory

A complete noise analysis of a copier + PSA cascaded system should be based on quantum theory [16–18]. However, a semi-classical description with satisfying accuracy is usually easier to grasp for the engineer. In this section, we will demonstrate how to model the noise characteristics of a non-degenerate, cascaded PSA amplified system in a semi-classical way.

As is well known, the general input-output (IO) relation of a non-degenerate (two-mode) parametric amplifier can be obtained in the undepleted-pump approximation [13,16]:

$$\begin{bmatrix} A_s \\ A_i^* \end{bmatrix} = \begin{bmatrix} \mu & \nu \\ \nu^* & \mu^* \end{bmatrix} \begin{bmatrix} A_{s0} + n_s \\ A_{i0}^* + n_i^* \end{bmatrix} = \mathbf{G} \cdot \begin{bmatrix} A_{s0} + n_s \\ A_{i0}^* + n_i^* \end{bmatrix}, \quad (1)$$

where A represents the complex amplitude, subscripts s and i denote signal and idler waves, respectively, A_{s0} is the input signal amplitude, and superscript $*$ represents the conjugation operation. The complex transfer coefficients μ and ν depend on the pump and the phase-matching conditions, as defined in Ref [13], and they also satisfy the auxiliary equation $|\mu|^2 - |\nu|^2 = 1$. Equation (1) applies to both PI- and PS-FOPAs with single- or dual-pumping. In this paper we only consider the co-polarized pump-signal-idler case to achieve the maximal performance [18]. The semi-classical expression of the uncorrelated vacuum

noise fields at the signal and idler frequencies are denoted by n_s and n_i , respectively. The statistics of the vacuum noise is assumed to be complex Gaussian, so that $\langle n_{s,i} \rangle = 0$, $\langle n_{s,i}^2 \rangle = 0$ and $\langle |n_{s,i}|^2 \rangle = hv_{s,i}/2$ [19], where $\langle \cdot \rangle$ denotes the expectation operation, h is the Planck constant and ν is the optical frequency. For simplicity, we only take into account the amplified vacuum noise rather than other noise contributions such as pump-transferred noise [19] and Raman phonon-seeded excess noise [20]. Subsequently, the attenuation process in the transmission fiber can be modeled semi-classically as [21,22]

$$\begin{bmatrix} A_s \\ A_i^* \end{bmatrix} = \hat{\mathbf{T}} \cdot \begin{bmatrix} A_{s0} + n_s \\ A_{i0}^* + n_i^* \end{bmatrix}, \quad (2)$$

and

$$\hat{\mathbf{T}} \cdot \mathbf{A} = \begin{bmatrix} \sqrt{T_s} & 0 \\ 0 & \sqrt{T_i} \end{bmatrix} \mathbf{A} + \begin{bmatrix} \sqrt{1-T_s} n_s' \\ \sqrt{1-T_i} n_i'^* \end{bmatrix},$$

where $\hat{\mathbf{T}}$ represents the attenuation operator, which behaves like a 4-port beam-splitter coupling the vacuum fields to the signal and the idler, and \mathbf{A} denotes the signal and idler field vector. The fiber transmittance is denoted by T , and n' represents the newly-introduced uncorrelated vacuum fluctuations associated with the loss process. In addition, a relative phase shift between the signal and idler will generally be induced by the residual dispersion of the fiber link unless perfect dispersion compensation is performed, which means that additional phase shifts for signal and idler waves, $e^{j\phi_s}$ and $e^{j\phi_i}$, should be imposed on the signal and idler fields, respectively. Similar to Eq. (1), the input-output (IO) relation of the PSA stage is

$$\begin{bmatrix} A_s \\ A_i^* \end{bmatrix} = \begin{bmatrix} e^{j\phi_s} & 0 \\ 0 & e^{-j\phi_i} \end{bmatrix} \begin{bmatrix} A_{s0} + n_s \\ A_{i0}^* + n_i^* \end{bmatrix} = \mathbf{D} \cdot \begin{bmatrix} A_{s0} + n_s \\ A_{i0}^* + n_i^* \end{bmatrix}, \quad (3)$$

where \mathbf{D} represents the phase shift induced by the transmission link and other devices. In Fig. 1, we show a simple schematic including three different operators (\mathbf{G} , $\hat{\mathbf{T}}$ and \mathbf{D}). Based on Eqs. (1)–(3), the output signal and noise fields can be obtained.

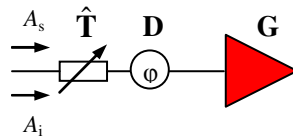


Fig. 1. Schematic of a non-degenerate PSA with loss and phase-shifter.

To analyze the noise performance of the transmission system, we choose the NF as an evaluating factor, since it is general and straightforward. According to [16], identical NF results are obtained for different detection methods (direct- or homodyne-detection) under the large-photon number approximation. For simplicity we only consider direct-detection here. Thus the signal NF will be

$$NF = \frac{SNR_{in}}{SNR_{out}} = \frac{\langle I_{in} \rangle^2 / \langle \Delta I_{in}^2 \rangle}{\langle I_{out} \rangle^2 / \langle \Delta I_{out}^2 \rangle}, \quad (4)$$

where SNR is the signal-to-noise ratio, and $I = R_0 |A_s|^2 B_0$ denotes the photocurrent after square-law detection. Here $R_0 = q / h\nu$ is the responsivity of an ideal photo-detector, with q being the electron charge, B_0 the optical bandwidth, and $\Delta I = I - \langle I \rangle$. In the next section we will apply this theory to cascaded links.

3. NF derivation for an m -span fiber link with cascaded copier + PSA inline amplification

We will now consider a multi-span fiber transmission system with periodic in-line discrete amplification. Two different link structures can be adopted for different applications, which are defined as Type A and Type B links throughout this paper. Generally, the Type A link which places the in-line amplifier in front of the transmission fiber is more suitable for conditions requiring higher SNR, while Type B scheme which amplifies the signal after the fiber link, is better for those applications where lower nonlinearity is necessary. Both types of link employ a copier + PSA cascaded in-line amplification, as shown in Fig. 2.

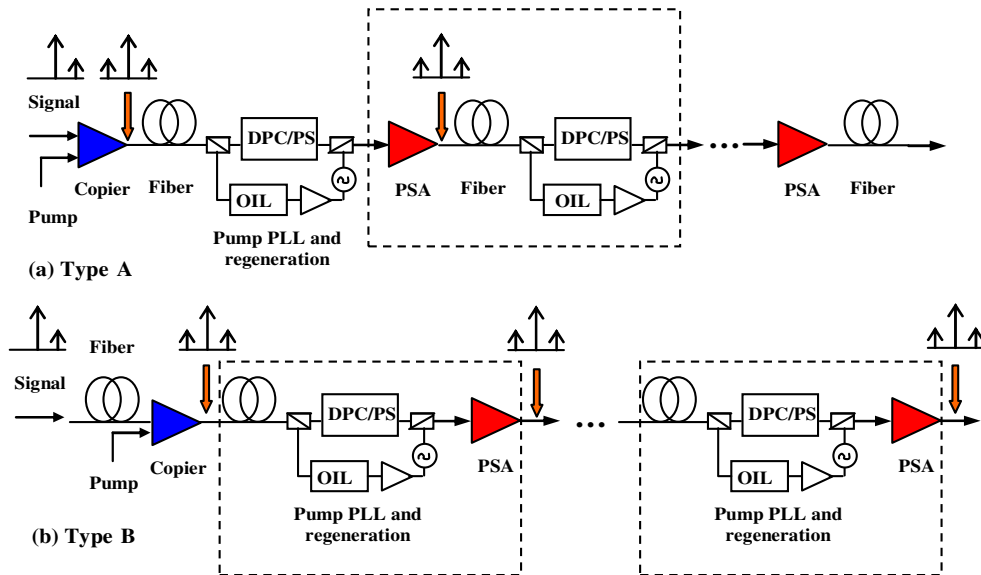


Fig. 2. (a) Type A and (b) Type B copier + PSA amplified multi-span transmission link. DPC/PC: Dispersion and polarization compensation / Phase shifter; OIL: Optical injection-locked laser; PLL: Phase locking loop.

Here, a PI-FOPA is used as the copier in the first span (amplifier + fiber), to amplify the signal as well as to generate the conjugated idler [9,13]. After the first span, the phase- and wavelength-locked signal, idler and pump waves will be input to the following parametric amplifiers, where non-degenerate PS amplification can be achieved. However, to achieve optimal PSA performance (highest gain and lowest NF), several practical issues need to be addressed: (i) The pump power and phase (propagated along the fiber as a pilot tone) must be regenerated with very low phase and intensity noise. This might be realized by using injection locking with a high performance slave laser [23,24]. (ii) The relative phase between the pump, signal and idler should be precisely manipulated to get the maximal PS gain, thus requiring perfect dispersion and dispersion slope compensation plus accurate phase-shifting. The simplest method is to use a piece of SMF with proper length [9]. However, for WDM applications, per-channel phase control is needed. Liquid-crystal [25] or MEMS [26] based frequency-resolved phase shifters might be good choices in such a situation. (iii) Polarization tracking and adaptive control are required at the input of each FOPA since parametric amplification is highly polarization-dependent [27]. (iv) Phase locking might be required for recombining the regenerated pump and the signal/idler wave before the PSAs, as shown in Fig. 2, to cancel the slowly-varying phase-errors induced by environmental fluctuations or

temperature changes. Of course the system performance will be much better if the above functions can be integrated together.

By assuming that the aforementioned four requirements have all been fulfilled, in the following we will analyze the noise performance of both Type A and B transmission systems with m transparent spans (fiber loss is exactly compensated by the amplifier gain).

3.1 Type A link

First, when $m = 1$, we have the IO relation according to Eqs. (1)–(3) as

$$\begin{bmatrix} A_{s,1} \\ A_{i,1}^* \end{bmatrix} = \hat{\mathbf{L}}_{A,1} \cdot \begin{bmatrix} A_{s0} + n_s \\ n_i^* \end{bmatrix} = \begin{bmatrix} \sqrt{T_{s,1}} \mu e^{j\varphi_{s,1}} & \sqrt{T_{s,1}} \nu e^{j\varphi_{s,1}} \\ \sqrt{T_{i,1}} \nu^* e^{-j\varphi_{i,1}} & \sqrt{T_{i,1}} \mu^* e^{-j\varphi_{i,1}} \end{bmatrix} \begin{bmatrix} A_{s0} + n_s \\ n_i^* \end{bmatrix} + \begin{bmatrix} \sqrt{1-T_{s,1}} n_{s,1}' e^{j\varphi_{s,1}} \\ \sqrt{1-T_{i,1}} n_{i,1}'^* e^{-j\varphi_{i,1}} \end{bmatrix}, \quad (5)$$

where $\hat{\mathbf{L}}_A = \mathbf{D}\hat{\mathbf{T}}\mathbf{G}$ is the link operator for the Type A system, the subscript 1 denotes the first span, which also applies to the elements in the phase-shift matrix \mathbf{D} , the attenuation operator $\hat{\mathbf{T}}$ and the parametric gain matrix \mathbf{G} . Actually, after the PIA, the signal and idler output powers are not perfectly equalized since the signal gain ($G_{s,1} = |\mu_1|^2 = G$) is not equal to the idler gain ($G_{i,1} = |\nu_1|^2$). To realize a transparent transmission for both signal and idler, we assume that $T_{s,1} = 1 / G_{s,1}$ and $T_{i,1} = 1 / G_{i,1}$ in the first span (to simplify the analysis, however, it will not affect the conclusion significantly if signal and idler experience identical loss), which can be practically made by using a gain equalization filter. Thus after the first span, we assume that exactly balanced signal and idler power levels are launched into the following PSAs. Based on Eq. (5) and the method used in Ref [28], and in the large-signal-photon-approximation, the output signal photocurrent and noise power are

$$\begin{aligned} \langle I_{out,1} \rangle &= R_0 G T |A_{s0}|^2 B_o = R_0 |A_{s0}|^2 B_o, \\ \langle \Delta I_{out,1}^2 \rangle &= 4R_0^2 |A_{s0}|^2 [2T(G-1)+1] h\nu \Delta f / 2. \end{aligned} \quad (6)$$

where Δf is the electrical receiver bandwidth. Here we neglected the noise-noise beat term, which is reasonable under the large-photon-number approximation. By combining Eqs. (4) and (6), we find the signal NF of the first span to be $NF_1 = 3 - 2/G$, which is consistent with the well-known PIA noise theory [14]. When the signal gain is much larger than 1, the NF expression can be reduced to $NF_{A,1} \approx 3$ (4.8 dB).

Subsequently, for two spans, $m = 2$, we have the IO relation as

$$\begin{bmatrix} A_{s,2} \\ A_{i,2}^* \end{bmatrix} = \hat{\mathbf{L}}_{A,2} \hat{\mathbf{L}}_{A,1} \cdot \begin{bmatrix} A_{s0} + n_s \\ n_i^* \end{bmatrix}. \quad (7)$$

Since both signal and idler are input into the second parametric amplifier, the signal gain will become phase-dependent [29]. It can be shown that the maximum PS gain for both signal and idler will be simultaneously obtained when the phase shift of the first span satisfy $\phi_{\mu 1} + \phi_{\mu 2} + \phi_{\nu 1} - \phi_{\nu 2} + \varphi_{s,1} + \varphi_{i,1} = 2n\pi$, $n = 0, 1, 2, \dots$, where $\phi_{\mu, \nu}$ represents the phase angles of the transfer coefficients μ and ν , respectively [30]. The maximal PS gain is

$$G_{s,2}(2n\pi) = G_{i,2}(2n\pi) = (|\mu_2| + |\nu_2|)^2 \approx 4|\mu_2|^2, \quad (8)$$

which means that both signal and idler will experience the same gain in the PSA, due to the balanced input powers, and this is also true for the following PSA stages. Thus for a transparent transmission link we have $T_{s,2} = T_{i,2} = 1 / G_{s,2}$. By assuming that the signal gain in each span is identical ($G = G_{s,1} = G_{s,2}$ and $T = T_{s,1} = T_{s,2}$), from Eq. (7) we have

$$\begin{aligned} \langle I_{out,2} \rangle &= R_0 (GT)^2 |A_{s0}|^2 B_o = R_0 |A_{s0}|^2 B_o, \\ \langle \Delta I_{out,2}^2 \rangle &= 4R_0^2 |A_{s0}|^2 [3 + (2|\mu_2|^2 - 1)T - 2|\mu_2|^2 T^2 - T] h\nu \Delta f / 2. \end{aligned} \quad (9)$$

By combining Eqs. (4) and (9), the approximate NF expression for an optimized two-span copier + PSA link can be derived as $NF_{A,2} \approx \frac{7}{2} - \frac{3T}{2}$, which will be further reduced to 7/2 (5.4 dB) in the high-gain regime, where $G = 1/T \gg 1$.

Now extending the above analysis to an m -span system, we have the IO relation as

$$\begin{bmatrix} A_{s,m} \\ A_{i,m}^* \end{bmatrix} = \hat{\mathbf{L}}_{A,m} \cdots \hat{\mathbf{L}}_{A,2} \hat{\mathbf{L}}_{A,1} \cdot \begin{bmatrix} A_{s0} + n_s \\ n_i^* \end{bmatrix}. \quad (10)$$

We can find that the maximal PS gain for both signal and idler can be obtained in the l -th ($1 < l \leq m$) span if the phase shift of the previous span satisfies the condition

$$\phi_{\mu,l-1} + \phi_{\mu,l} + \phi_{\nu,l-1} - \phi_{\nu,l} + \phi_{s,l-1} + \phi_{i,l-1} = 2n\pi, n = 0, 1, 2, \dots, \quad (11)$$

which means that the relative phase of each PSA can be optimized independently. Similarly, by assuming the signal gain in each span is identical ($G = G_{s,1} = G_{s,2} = \dots = G_{s,m}$ and $T = T_{s,1} = T_{s,2} = \dots = T_{s,m}$), and only considering the optimal condition, the elements in the link operator $\hat{\mathbf{L}}_{A,l}$ ($l \geq 2$) can be replaced by their modules as

$$\begin{bmatrix} A_{s,l} \\ A_{i,l}^* \end{bmatrix} = |\hat{\mathbf{L}}_{A,l}| |\hat{\mathbf{L}}_{A,l-1}| \cdots |\hat{\mathbf{L}}_{A,2}| |\hat{\mathbf{L}}_{A,1}| \cdot \begin{bmatrix} A_{s0} + n_s \\ n_i^* \end{bmatrix}, \quad (12)$$

where

$$|\hat{\mathbf{L}}_{A,l}| \begin{bmatrix} A_s + n_s \\ A_i^* + n_i^* \end{bmatrix} = \sqrt{T} \begin{bmatrix} |\mu_2| & |v_2| \\ |v_2| & |\mu_2| \end{bmatrix} \cdot |\hat{\mathbf{L}}_{A,l-1}| \cdots |\hat{\mathbf{L}}_{A,2}| |\hat{\mathbf{L}}_{A,1}| \cdot \begin{bmatrix} A_{s0} + n_s \\ A_i^* + n_i^* \end{bmatrix} + \sqrt{1-T} \begin{bmatrix} n_{s,l} \\ n_{i,l} \end{bmatrix},$$

to simplify the calculations. However, the exact NF expression for an m -span copier + PSA amplified system is still too long to show here. By noting that $|\mu_2|^2 + |v_2|^2 = (|\mu_2| + |v_2|)^2 + (|\mu_2| - |v_2|)^2 / 2$, and assuming that the copier operates in the high-gain regime (where $|\mu_1| \approx |v_1|$), a reduced output expression can be derived as

$$\begin{aligned} \langle I_{out,m} \rangle &= R_0 (GT)^m |A_{s0}|^2 B_o = R_0 |A_{s0}|^2 B_o, \\ \langle \Delta I_{out,m}^2 \rangle &\approx 4R_0^2 |A_{s0}|^2 [3 - T + \sum_{i=2}^m (\frac{G^{i-1} + T^{i-1}}{2}) T^{i-1} (1 - T)] h\nu \Delta f / 2. \end{aligned} \quad (13)$$

By combining Eqs. (8) and (13) and assuming $T \ll 1$, we obtain the approximate NF formula

$$NF_{A,m} \approx \frac{5}{2} + \frac{m}{2}. \quad (14)$$

3.2 Type B link

For a Type B link, some minor modifications to the above analysis are needed. When $m = 1$, we have

$$\begin{bmatrix} A_{s,1} \\ A_{i,1}^* \end{bmatrix} = \hat{\mathbf{L}}_{B,1} \cdot \begin{bmatrix} A_{s0} + n_s \\ n_i^* \end{bmatrix} = \begin{bmatrix} \sqrt{T_{s,1}} \mu_1 & \sqrt{T_{s,1}} \nu_1 \\ \sqrt{T_{i,1}} \nu_1^* & \sqrt{T_{i,1}} \mu_1^* \end{bmatrix} \begin{bmatrix} A_{s0} + n_s \\ n_i^* \end{bmatrix} + \begin{bmatrix} \sqrt{1-T_{s,1}} \mu_1 n_{s,1}' + \sqrt{1-T_{i,1}} \nu_1 n_{i,1}'^* \\ \sqrt{1-T_{s,1}} \nu_1^* n_{s,1}' + \sqrt{1-T_{i,1}} \mu_1^* n_{i,1}'^* \end{bmatrix}, \quad (15)$$

where $\hat{\mathbf{L}}_B = \mathbf{GDT}$ is the link operator for the Type B link. For the first stage, since there is no idler propagating in the fiber, for simplicity we assume the phase shift $\varphi_{s,1}$ and $\varphi_{s,12}$ are zero and the fiber loss is identical for signal and idler waves, which compensates the signal PIA gain ($G_{s,1} = |\mu_1|^2 = G$ and $T_{s,1} = T_{i,1} = 1/G$). In the same way, we have

$$\begin{aligned} \langle I_{out,1} \rangle &= R_0 GT |A_{s0}|^2 B_o = R_0 |A_{s0}|^2 B_o, \\ \langle \Delta I_{out,1}^2 \rangle &= 4R_0^2 GT |A_{s0}|^2 [T(2G-1) + (1-T)(2G-1)] h\nu \Delta f / 2. \end{aligned} \quad (16)$$

By using Eq. (4), we obtain the signal NF of the first span as $NF_{B,1} = 2G - 1$, which will reduce to $NF_{B,1} = 2G$ when the gain is large.

When $m = 2$, we have the IO relation as

$$\begin{bmatrix} A_{s,2} \\ A_{i,2}^* \end{bmatrix} = \hat{\mathbf{L}}_{B,2} \hat{\mathbf{L}}_{B,1} \cdot \begin{bmatrix} A_{s0} + n_s \\ n_i^* \end{bmatrix}. \quad (17)$$

To realize balanced transmission for signal and idler, we assume that $T = T_{s,2} = 1/G$ and $T_{i,2} = 1/(G-1)$ in the second span, and thus exactly equalized signal and idler powers can be provided for the following PSAs, as shown in the previous sub-section. The maximal PS gain can be obtained by optimizing the phase shift of the second span to satisfy $\phi_{\mu 1} + \phi_{\mu 2} + \phi_{\nu 1} - \phi_{\nu 2} + \varphi_{s,2} + \varphi_{i,2} = n\pi$, $n = 0, 1, 2, \dots$. According to Eq. (17), we have

$$\begin{aligned} \langle I_{out,2} \rangle &= R_0 (GT)^2 |A_{s0}|^2 B_o = R_0 |A_{s0}|^2 B_o, \\ \langle \Delta I_{out,2}^2 \rangle &= 4R_0^2 GT |A_{s0}|^2 [2G + 2|\mu_2|^2 - 2|\mu_2|^2 T - 1] h\nu \Delta f / 2. \end{aligned} \quad (18)$$

If the amplifiers are assumed to have high gain (i.e. $T \ll 1$), the approximate NF expression of an optimized two-span copier + PSA link is $NF_{B,2} \approx \frac{5G}{2} - \frac{1}{2}$, by using Eqs. (4) and (18), which means that Type B will lead to a much larger NF due to the large fiber losses placed before the amplifiers.

After the second span, the maximal signal and idler gains will be the same in the following PSAs. Assuming that the copier gain is much larger than 1 (i.e. $|\mu_1| \approx |\nu_1|$) and following the procedure described in Section 3.1, we have

$$\begin{aligned} \langle I_{out,m} \rangle &= R_0 (GT)^m |A_{s0}|^2 B_o = R_0 |A_{s0}|^2 B_o, \\ \langle \Delta I_{out,m}^2 \rangle &\approx 4R_0^2 |A_{s0}|^2 \left[2G + \sum_{i=2}^m \left(\frac{G^{i-1} + T^{i-1}}{2} \right) T^{i-2} (1-T) \right] h\nu \Delta f / 2. \end{aligned} \quad (19)$$

Therefore the approximate NF formula (at the maximal PSA gain) can be derived as

$$NF_{B,m} \approx \frac{3G}{2} + \frac{mG}{2}. \quad (20)$$

4. Comparison and discussion

The noise performance of pure-PIA and pure-PSA amplified links have been extensively studied. For the PIA case, under the large-photon-number assumption, the total NFs of an m -span transparent fiber link can be expressed as [14–17]

$$\begin{aligned} NF_{A,m} &= 1 + 2m(1 - 1/G), \\ NF_{B,m} &= 1 + 2mG(1 - 1/G), \end{aligned} \quad (21)$$

for the Type A and Type B schemes, respectively, where G is the amplifier gain in each span. In fact the above results can also be derived for PI-FOPAs based on Eqs. (1)–(4), as demonstrated in Appendix A.

For the pure-PSA case, both degenerate and non-degenerate PSAs should be considered. In Ref [15,16], pure degenerate PSA in-line amplification was investigated, which shows that the optimal m -span NFs could be expressed as

$$\begin{aligned} NF_{A,m} &= 1 + m(1 - 1/G), \\ NF_{B,m} &= 1 + mG(1 - 1/G), \end{aligned} \quad (22)$$

for the Type A and Type B links, respectively. We can also derive Eq. (22) through Eqs. (1)–(4) by assuming that the signal and idler always have the same field and occupy the same wavelength, as shown in Appendix B. However, for a pure non-degenerate PSA amplified transmission system, things become more complicated since there are two input waves. When calculating or measuring the NF, it is necessary to take into account signal and idler launched powers of a non-degenerate PSA together as the actual input power because both waves should carry information. In fact, a non-degenerate PSA in which only one of the inputs carries data is not suitable for in-line amplification. Based on this, the derived optimal NF will be 0 dB at high gain (otherwise the minimal NF will be -3 dB when considering the signal or idler alone), as mentioned in Refs [13,16]. In Appendix B, the optimized NFs of an m -span non-degenerate PSA link are obtained as $NF_{A,m} \approx 2 + m$ and $NF_{B,m} \approx mG$, for both Type A and B cases. Thus we see that the non-degenerate schemes have the same SNR performance as the degenerate ones in the long-haul, high gain limit.

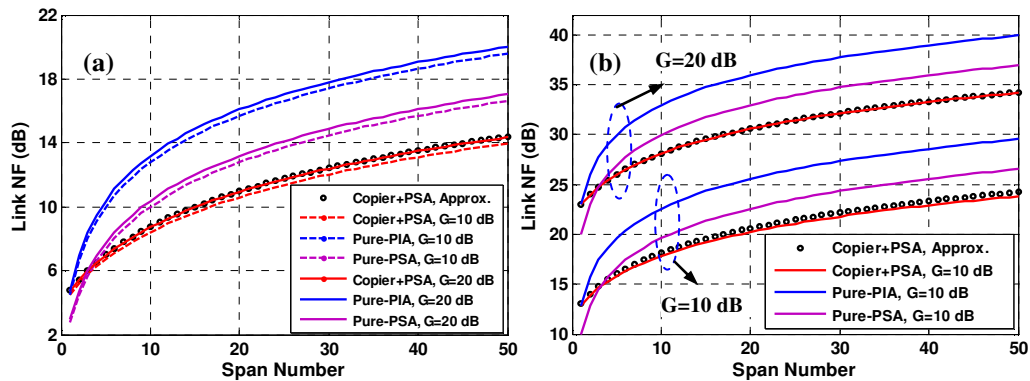


Fig. 3. Calculated (a) Type A link NF and (b) Type B link NF vs. the span number for the cascaded copier + PSA, pure-PIA and pure-PSA transmission systems at different link gains. Black circles shows the approximate results based on Eqs. (14) and (20), respectively.

Comparing Eqs. (14) and (20) to Eqs. (21) and (22), we obtain the surprising result that for high gain and large span numbers, the NF of a copier + PSA amplified system (either Type A or B) will be 6 dB or 3 dB better than that of a pure-PIA or pure-PSA links. In Figs. 3(a) and 3(b), we show the NF curves (as functions of the span number) for the three different links

with Type A and B configurations, respectively, which demonstrate that a copier + PSA link will have lower NF than a pure-PSA link when $m > 3$, and a 2-dB NF improvement will be observed compared with the pure-PIA case when $m = 2$. It should be noted that Eqs. (14) and (20) will give a good NF estimate when the link gain is larger than 10 dB.

A qualitative explanation for this counter-intuitive performance improvement when using the copier relies on two important points. First, in a long-haul transmission system with many spans, most of the noise is induced by the fiber loss, and the noise contribution from the first PI-FOPA will become less important. Secondly, for such a cascaded copier + PSA link, only the signal wave should be considered when calculating the NF (as there is no idler at the link input), thus the NFs of the following PSAs can be regarded to be -3 dB [16] when the fiber loss is substantial (assuming uncorrelated inputs into each PSA). The reason why the NF of a pure-PSA link is 3 dB worse than that of a cascaded copier + PSA one is that the former scheme uses twice the input power, comprising both the signal and idler waves.

To the best of our knowledge, the copier + PSA in-line amplification will provide the lowest NF for any long-haul transmission system with discrete amplifiers, and this conclusion is also true for systems with distributed amplification. For example, considering an m -span transparent distributed copier + PSA link with uniform pump power along the fiber, as described in Ref [13], for the first span the NF is $1 + 2 \ln G$, which is the ideal NF of a distributed PIA. Then the following distributed PSA spans will give an approximate minimal NF of $0.5 \ln G$ by only taking into account the signal input [13], which is exactly the same case for the cascaded copier + PSA scheme. Therefore, compared with the pure-PIA distributed amplification ($1 + 2m \ln G$) and the pure-PSA case ($1 + m \ln G$), the same asymptotic 6 dB or 3 dB NF improvement can be expected by using the cascaded copier + PSA distributed amplification. A more advanced analysis based on quantum theory is required to fully evaluate the noise performance of a distributed copier + PSA link.

It is also interesting to compare the spectral efficiencies of different transmission links. Compared with the pure-degenerate-PSA amplified system, the cascaded copier + PSA can carry twice as much information within a doubled bandwidth, since the idler generated from the first stage carries the conjugated signal phase information, which means that any phase state of the input signal can be amplified in the following PSAs, and not only a specific quadrature. Compared with the pure-non-degenerate-PSA amplified system, in principle they have the same spectral efficiency, since a non-degenerate PSA also has the potential to encode information on two quadratures [13], however, more complicated processing and detection methods to simultaneously measure the signal and idler fields might be required. On the other hand, compared with the pure-PIA (e.g. EDFAs and Raman amplifiers) amplified link, the copier + PSA scheme will have a 3-dB lower spectral efficiency, since the idlers do propagate along the link occupying spectral space (not necessarily near the signal). Thus the 6 dB NF improvement in long-haul systems comes at the price of halved spectral efficiency. A wide band FOPA [31] will compensate this spectral inefficiency to some extent, since it will provide more gain bandwidth compared to conventional amplifiers. In addition, the accompanying idler can also be used in other applications such as wavelength conversion.

We should emphasize that in the above discussions we only considered the fundamental amplified quantum noise. In fact other noise contributions exist in FOPAs [32] such as the pump transferred noise and Raman phonon-seeded excess noise, as previously mentioned. The former contribution can be effectively suppressed by using a clean pump as well as a lower signal power, while the latter one can be canceled by adopting a cross-polarized pump-signal/idler scheme [13]. In a properly designed FOPA, it is reasonable to assume the excess NF induced by these two noise sources will be less than 1 dB.

5. Experimental proof of concept

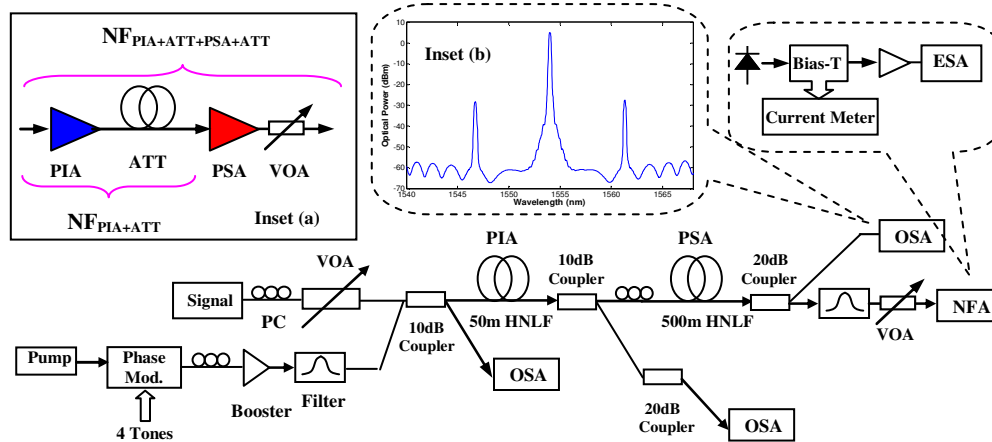


Fig. 4. Experimental setup. NFA: Noise figure analyzer; ESA: Electrical spectrum analyzer; OSA: Optical spectrum analyzer; PC: Polarization controller; VOA: Variable optical attenuator. Inset (a) shows the principal scheme and inset (b) shows the output optical spectrum.

As a proof of concept, we measured the NF of a PI-FOPA + attenuator (ATT) + PS-FOPA + ATT cascade to resemble the two-span copier + PSA amplified transmission link. Figure 4 shows the experimental setup. A 60-mW low-noise DFB laser (1554.4 nm) was used as the pump laser, which was phase-modulated to suppress stimulated Brillouin scattering. After an 8.5 W EDFA booster followed by two cascaded 2-nm filters, the amplified pump was combined with signal by a 10-dB coupler representing the transmission fiber loss. Two spools (50 m and 500 m each) of highly nonlinear fibers (HNLF, parameters are $\lambda_0 = 1552$ nm, $\gamma = 11.8$ W⁻¹km⁻¹ and $S_0 = 0.02$ ps/nm²·km) were used as the PIA and PSA, respectively. In between the two stages, another SMF-based 10 dB coupler (SMF length = 7 m) was inserted as the mid-stage attenuator as well as the signal/idler/noise monitor. In the linear regime, this 10dB coupler can be viewed as a 50 km transmission fiber with dispersion compensation. We connected the 10% port to the PSA input. A 20 dB coupler was spliced after the PSA to monitor the output spectrum, and two cascaded filters were used to effectively filter out the residual pump and the amplified noise. By choosing this setup, no phase-locked loops are needed, which makes it possible to measure the NF in a more stable condition. Finally the amplified signal and idler were properly attenuated and then detected by the NF analyzer. The detected signal and noise components were separated by a bias-T, and then measured by a current meter and electrical spectrum analyzer, respectively. After carrying out calibration for shot noise and subtracting laser relative-intensity-noise (RIN) [30,33], the NF can be obtained from the following equation

$$NF = \frac{1}{G} + \frac{P_{in}(S_{out} - S_{in})}{2hvI_{out}^2}, \quad (23)$$

where P_{in} is the input signal power, S_{out} and S_{in} are the noise power spectral density measured at the input and output of the amplifier, respectively, and I_{out} is the detected output signal photocurrent. According to Eq. (20), the NF of a transparent amplifier + ATT cascade can be easily derived by measuring S_{out} , S_{in} and I_{out} at a proper signal-power level and then replacing the net gain G with 0 dB in Eq. (23). We chose 894.7 MHz as the central frequency to measure the noise power spectral density, with 2-MHz resolution bandwidth and 3-Hz video bandwidth. In most cases, the NF measurement error is within ± 0.4 dB. The output noise

spectrum of the PSA is shown in inset (b) of Fig. 4, which clearly shows that the PSA gain changes with the relative phase.

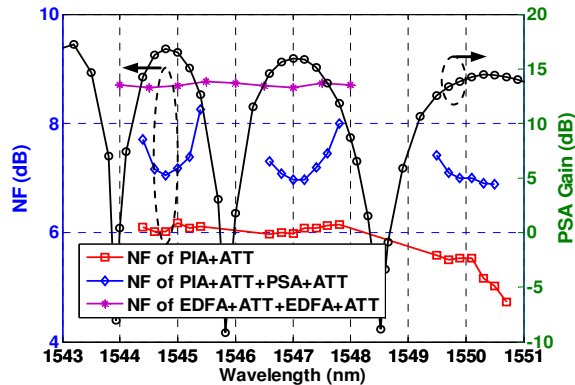


Fig. 5. Measured PSA gain and NF spectra of different cascaded amplification cases.

In our setup, 10-dB average PIA gain was achieved in the first (copier) stage to realize transparent amplification, which leads to well equalized signal and idler inputs to the PSA. The maximal PSA gain at 1561.7 nm is larger than 16 dB. The average input signal power is -19.4 dBm to reduce the pump-noise transfer. Figure 5 shows the measured copier, PSA gain spectra as well as the NF spectra of the copier + ATT cascade (representing the one-span link) and the copier + ATT + PSA + ATT cascade (representing the two-span link). At the peak PSA gain around 1561.7 nm, $NF_{PIA+ATT+PSA}$ is very close or even slightly lower than $NF_{PIA+ATT}$, indicating the noise benefit from the PSA stage. The total NF degradation close to the pump is due to the strong pump residual ASE noise-induced measurement errors. For comparison, we also measured the NF of an EDFA + ATT + EDFA + ATT cascade (total NF is about 8.8 dB). The NF as well as the net gain of the EDFA + ATT part was almost equal to that of the copier + ATT case (with about 6 dB NF and 0 dB net gain, respectively), while the second EDFA had a 4.5 dB NF. The results show that under the above conditions, the cascaded FOPA has a 1.8-dB NF advantage over the conventional cascaded EDFA scheme, which is consistent with the theoretical predictions. Larger benefits can be expected for larger PSA span numbers, however, pump power and phase regeneration is then required.

6. Conclusion

The noise performance of a multi-span fiber optical transmission link employing the cascaded copier + PSA scheme for in-line amplification was investigated based on semi-classical theory. Compared with the pure-PIA and the pure-PSA based links, the cascaded copier + PSA scheme can improve the system NF by up to 6 and 3 dB, respectively. This scheme might be more economically feasible and thus more promising for long-haul transmissions since it will significantly loosen the requirement for accurate phase- and wavelength-locking which is rigorously needed for the pure-PSA case. As a proof of concept, the NF of a copier + PSA cascade with an inter-stage attenuation representing the fiber link was measured, which showed a 1.8 dB total NF improvement over a conventional cascaded EDFA scheme. Larger improvements can be expected if more PSA stages are added.

Appendix A: NF derivation of the pure-PIA link

Minor modifications are required to model the PI-FOPA-only link based on semi-classical theory, and the results can be generalized to more conventional PIAs like EDFAs. The difference between the copier + PSA link and the PIA-only link is that there is no idler at the

input of each span. To model this, we introduce the modified link operators $\hat{\mathbf{L}}_{A,PIA} = \hat{\mathbf{K}}\hat{\mathbf{T}}\mathbf{G}$ and $\hat{\mathbf{L}}_{B,PIA} = \hat{\mathbf{K}}\mathbf{G}\hat{\mathbf{T}}$, for Type A and Type B links respectively, where \mathbf{D} is replaced by

$$\hat{\mathbf{K}} \begin{bmatrix} A_{s0} + n_s \\ A_{i0}^* + n_i^* \end{bmatrix} = \begin{bmatrix} 1 & 0 \\ 0 & 0 \end{bmatrix} \begin{bmatrix} A_{s0} + n_s \\ A_{i0}^* + n_i^* \end{bmatrix} + \begin{bmatrix} 0 \\ n_i^* \end{bmatrix},$$

which is the operator that completely kills the idler after each span (The phase condition is not important in a phase-insensitive link.) Thus, we have the following IO relations

$$\begin{aligned} \begin{bmatrix} A_{s,m} \\ A_{i,m}^* \end{bmatrix} &= \hat{\mathbf{L}}_{A,PIAm} \cdots \hat{\mathbf{L}}_{A,PIA2} \hat{\mathbf{L}}_{A,PIA1} \cdot \begin{bmatrix} A_{s0} + n_s \\ n_i^* \end{bmatrix}, \\ \begin{bmatrix} A_{s,m} \\ A_{i,m}^* \end{bmatrix} &= \hat{\mathbf{L}}_{B,PIAm} \cdots \hat{\mathbf{L}}_{B,PIA2} \hat{\mathbf{L}}_{B,PIA1} \cdot \begin{bmatrix} A_{s0} + n_s \\ n_i^* \end{bmatrix}. \end{aligned} \quad (24)$$

By assuming that the fiber link is transparent ($T = 1/G$ in each span), we have

$$\langle \Delta I_{out,m}^2 \rangle = 4R_0^2 |A_{s0}|^2 \left[1 + \sum_{i=1}^m 2(1-T) \right] h\nu \Delta f / 2, \quad (25)$$

for a Type A link and

$$\langle \Delta I_{out,m}^2 \rangle = 4R_0^2 |A_{s0}|^2 \left[1 + \sum_{i=1}^m 2G(1-T) \right] h\nu \Delta f / 2, \quad (26)$$

for a Type B link. By following the same analysis, we can obtain the same results as Eq. (21).

Appendix B: NF derivation of the pure-PSA link

First we consider degenerate PSA transmission systems. The IO relations of an m-span degenerate-PSA-amplified fiber link can be similarly modeled as

$$\begin{bmatrix} A_{s,m} \\ A_{s,m}^* \end{bmatrix} = \hat{\mathbf{L}}_{A,PSAm} \cdots \hat{\mathbf{L}}_{A,PSA2} \hat{\mathbf{L}}_{A,PSA1} \cdot \begin{bmatrix} A_{s0} + n_s \\ A_{s0}^* + n_s^* \end{bmatrix}, \quad (27)$$

for a Type A link, where $\hat{\mathbf{L}}_A = \mathbf{D}\hat{\mathbf{T}}\mathbf{G}$ has the same definition as used in section 3.1, and

$$\begin{bmatrix} A_{s,m} \\ A_{s,m}^* \end{bmatrix} = \hat{\mathbf{L}}_{B,PSAm} \cdots \hat{\mathbf{L}}_{B,PSA2} \hat{\mathbf{L}}_{B,PSA1} \cdot \begin{bmatrix} A_{s0} + n_s \\ A_{s0}^* + n_s^* \end{bmatrix}, \quad (28)$$

for a Type B link, where $\hat{\mathbf{L}}_B = \mathbf{G}\mathbf{D}\hat{\mathbf{T}}$. It should be noted that in the degenerate case, the signal and idler are actually the same field. Considering the optimal condition, i.e. $G = (|\mu| + |\nu|)^2$, and assuming transparent amplification, we have

$$\langle \Delta I_{out,m}^2 \rangle = 4R_0^2 |A_{s0}|^2 \left[1 + \sum_{i=1}^m (1-T) \right] h\nu \Delta f / 2, \quad (29)$$

for the Type A link and

$$\langle \Delta I_{out,m}^2 \rangle = 4R_0^2 |A_{s0}|^2 \left[1 + \sum_{i=1}^m G(1-T) \right] h\nu \Delta f / 2, \quad (30)$$

for the Type B link. By using Eq. (4), the same results as Eq. (22) can be obtained.

For the pure non-degenerate case, the IO relations become slightly different since the signal and idler are no longer the same wave. We have

$$\begin{bmatrix} A_{s,m} \\ A_{i,m}^* \end{bmatrix} = \hat{\mathbf{L}}_{A,PSAm} \cdots \hat{\mathbf{L}}_{A,PSA2} \hat{\mathbf{L}}_{A,PSA1} \cdot \begin{bmatrix} A_{s0} + n_s \\ A_{i0}^* + n_i^* \end{bmatrix}, \quad (31)$$

$$\begin{bmatrix} A_{s,m} \\ A_{i,m}^* \end{bmatrix} = \hat{\mathbf{L}}_{B,PSAm} \cdots \hat{\mathbf{L}}_{B,PSA2} \hat{\mathbf{L}}_{B,PSA1} \cdot \begin{bmatrix} A_{s0} + n_s \\ A_{i0}^* + n_i^* \end{bmatrix}, \quad (32)$$

for the Type A and Type B configurations, respectively. By noting that $|\mu_2|^2 + |\nu_2|^2 = [(|\mu_2| + |\nu_2|)^2 + (|\mu_2| - |\nu_2|)^2] / 2$, and only considering the signal wave, we have

$$\langle \Delta I_{out,m}^2 \rangle = 4R_0^2 |A_{s0}|^2 \left[1 - T + \left(\frac{G^m + T^m}{2} \right) T^m + \sum_{i=1}^{m-1} \left(\frac{G^i + T^i}{2} \right) T^i (1 - T) \right] h\nu \Delta f / 2, \quad (33)$$

for a Type A link, and

$$\langle \Delta I_{out,m}^2 \rangle = 4R_0^2 |A_{s0}|^2 \left[\left(\frac{G^m + T^m}{2} \right) T^m + \sum_{i=1}^m \left(\frac{G^i + T^i}{2} \right) T^{i-1} (1 - T) \right] h\nu \Delta f / 2, \quad (34)$$

for a Type B link. Moreover, since both signal and idler waves should be taken into account in the non-degenerate PSA case, a factor of 2 (3 dB) should be multiplied to the input SNR [13,34], while the output SNR remains identical, which will give the ‘real’ PSA NF in the high gain regime [13]. Thus by combing Eq. (4) and assuming $T \ll 1$, we have

$$\begin{aligned} NF_{As,m} &\approx m + 2, \\ NF_{Bs,m} &\approx mG. \end{aligned} \quad (35)$$

Acknowledgements

The research leading to these results received funding from the European Communities Seventh Framework Programme FP/2007-2013 under grant agreement 224547 (STREP PHASORS), and also from the Air Force Office of Scientific Research, Air Force Material Command, USAF, under grant number FA8655-09-1-3076. Z. Tong would like to thank Dr. Per-Olof Hedekvist for help with error analysis, Dr. Michael Vasilyev for enlightening help, Dr. Adonis Bogris, Dr. Andrew Ellis and Dr. Stylianos Sygletos for fruitful discussions.